PASJ: Publ. Astron. Soc. Japan **63**, 727–733, 2011 August 25
© 2011. Astronomical Society of Japan.

Can X-Ray Lasers Exist in Astrophysical Objects ?

David SALZMANN and Hideaki TAKABE
Institute for Laser Engineering, Osaka University, 2-6 Yamadaoka, Suita, Osaka 565-0871

(Received 2011 February 16; accepted 2011 March 28)

Abstract

We consider the possibility of population inversion in astrophysical objects irradiated by high-intensity black-body radiation from a nearby source. As a model, we use the $1s2p\,^1P_1$ populations in helium-like ions, which are generated by K-shell photoionization of lithium-like ions. Our conclusion is that the presently known highest astrophysical irradiation conditions are insufficient to produce population inversion for this transition. According to our estimate, population inversion is possible only in the visible or longer wavelength regimes. Our estimates may change for non-black-body radiation distributions.

Key words: atomic physics — photoionization — X-rays: binaries

1. Introduction

Masers and lasers generated by astrophysical objects in the microwave and IR regimes are well-established facts. In the present paper we investigate the possibility of similar lasing effects also in the UV or x-ray regimes.

An astrophysical maser has been discovered at 1670 MHz, originating from OH molecules near stars (Weaver et al. 1965). In the absence of cavities or mirrors, the amplification process of the radiation intensity is boosted in a single pass through a dense region of a molecular gas (Stahler & Palla 2004). Such regions, with their clusters of luminous spots, appear in the perturbed vicinity of young stars. Masers are also found in many other environments, including planetary atmospheres, stellar atmospheres, supernova remnants (Wardle & Yusef-Zadeh 2002), pulsars (Weisberg et al. 2005), and the external galaxies (Whiteoak & Gardner 1973; Nakai et al. 1993). In contrast, the optical analogue, namely an astrophysical laser, is more difficult to be observed, due to the shorter lifetime of the excited state and mixture with spontaneous emission. In fact, so far astrophysical lasers have not yet been reported. The closest to the visible is a report by Johansson and Letokhov, who found an astrophysical laser in spectral lines in the near IR, 0.9–2 μm (0.6–1.4 eV) in Weigelt blobs in the vicinity of η Carinae from data obtained with the HST/STIS facility (Johansson & Letokhov 2007). According to their analysis, the mechanism of population inversion is photoexcitation. Recently, Messenger and Strelnitski (2010) confirmed their suggestion, but proposed a different mechanism.

An experimental demonstration of lasing in the EUV regime was carried out at Sandia Laboratories (Porter et al. 1992), using sodium Z-pinch. Radiation from the He-like sodium $1s^2$–$1s2p\,^1P_1$ transition (11.0027 Å, 1126.85 eV) photoexcited the $1s^24p\,^1P_1$ state in He-like neon (11.0003 Å, 1127.10 eV above g.s.). Collisions transferred the excited ions to the 4 d and 4 f levels. Lasing was observed in the $1s3d\,^1D_2$–$1s4f\,^1F_1$ transition at 231 Å, 53.67 eV. To maximize the effect, the sodium plasma had high density (10^{19} ions cm^{-3}) and high temperature (300 eV). The radiative energy in the lasing line is, however, only a tiny fraction of the invested energy.

The necessary condition for lasing is population inversion. This, however, needs an external source that pumps energy into the system, and excites the lasing medium. To emit radiation in the x-ray energy range, the lasing material has to have an atomic number, Z, that is high enough to produce radiation in the UV or x-ray regimes. On the other hand, for a high-Z material the excited levels decay rapidly to the ground state, so that it is very difficult to maintain stable population inversion.

Natural candidates as astrophysical energy sources are compact objects (black hole, neutron star, or white dwarf) in binary systems, which emit huge amounts of high-temperature black-body (BB) radiation. This radiation hits the material ejected from the companion star toward the accretion disc, thereby generating a photoionizing plasma—a low temperature, but highly ionized medium. The spectral properties of such plasmas were thoroughly investigated both for astrophysical and laboratory plasmas, see for instance Remington, Drake, and Ryutov (2006) and Takabe (2001). Analysis of these spectra indicate a radiation temperature on the order of 0.5–2.0 keV, which generates highly ionized species (Li-, He-, and H-like ions for elements with atomic number as high as iron), even when the plasma electron temperature is as low as 10–50 eV. Another interesting property of photoionizing plasmas is the fact that only the K- or L-shells are populated, because low and intermediate-Z ions have a low fluorescence yield, and relaxation of an inner shell vacancy proceeds with high probability by means of radiationless transitions (Bambynek et al. 1972), in which electrons at higher shells are ejected through the Auger effect. In principle, there is also the possibility of atomic excitation by intense particle or electron beams, but as yet such phenomena have not been reported.

The atomic processes in photoionized plasmas are significantly different from those in collisional plasmas. For instance, while the production of excited ions in collisional plasmas is done mostly by electron impact excitation, dielectronic recombination or recombination cascade, the generation of such states in photoionized plasmas is also carried out by photoionization of inner-shell electrons, or by the direct photoexcitation of ground-state ions. However, while electron-collision effects generate a statistical distribution of the atomic excitation states,

Downloaded from https://academic.oup.com/pasj/article-abstract/63/4/727/2902469
by Institute of Botany, CAS user
on 17 November 2017

only photon-induced processes can generate an inverted population. Consequently, in our search for x-ray lasers in the Universe we are looking for photoionizing plasmas.

As a model for an atomic configuration that can be the basis for an x-ray laser, we consider the process in which a K-shell electron is photoionized in a ground state (g.s.) $1s^2\,2l$ ($l = s, p$) lithium-like ion, thereby generating an excited helium-like $1s\,2l$ ion. The species in the $1s\,2p\,^1P_1$ excited state, which have the highest Einstein A-coefficient, decay into a $1s^2\,^1S_0$ g.s. helium ion, either by spontaneous decay (in low radiation density fields) or by stimulated emission (in high density fields). Although this model considers only a very special atomic configuration, our treatment is general enough to apply to other atomic configurations as well.

Stimulated emission may occur only if the upper state is overpopulated, namely,

$$\frac{N_{\rm up}}{N_{\rm low}} > \frac{g_{\rm up}}{g_{\rm low}}, \tag{1}$$

where the g's are the statistical weights of the upper and lower levels. For the above transition this condition translates into

$$\frac{N(1s2p\,^1P_1)}{N(1s^2)} > \frac{3}{1} = 3. \tag{2}$$

2. The Stationary Point

To make this paper more readable, the mathematical details are shifted to the appendixes. In appendix 1 we develop the rate coefficients for the photoionization and photoexcitation effects. The rate equations that determine the population and depopulation rates of the $1s^2\,^1S_0$ ground state and the $1s\,2p\,^1P_1$ excited state are developed and explained in appendix 2. These equations have the form

$$\begin{pmatrix} dN_{\rm He,1}/dt \\ dN_{\rm He,2}/dt \end{pmatrix} = \begin{pmatrix} -a_{11} & a_{12} \\ a_{21} & -a_{22} \end{pmatrix} \begin{pmatrix} N_{\rm He,1} \\ N_{\rm He,2} \end{pmatrix} + \begin{pmatrix} b_1 \\ b_2 \end{pmatrix}, \tag{3}$$

where $N_{\rm He,1}$ and $N_{\rm He,2}$ are the densities of the ground $1s^2\,^1S_0$ and excited $1s\,2p\,^1P_1$ He-like ionic states, respectively. The a's and b's are functions of the rate coefficients of all possible ionic processes that populate and depopulate the two ionic levels (see explicit formulas in appendix 2). The stationary point, namely the condition at which the ground and excited states' populations are time-independent, is attained when

$$\frac{dN_{\rm He,1}}{dt} = \frac{dN_{\rm He,2}}{dt} = 0. \tag{4}$$

Inserting equation (4) into equation (3) one obtains the densities of the two states at stationary condition,

$$\begin{aligned} \begin{pmatrix} N_{1,0} \\ N_{2,0} \end{pmatrix} &= -\begin{pmatrix} -a_{11} & a_{12} \\ a_{21} & -a_{22} \end{pmatrix}^{-1} \begin{pmatrix} b_1 \\ b_2 \end{pmatrix} \\ &= \frac{1}{det} \begin{pmatrix} a_{22} & a_{12} \\ a_{21} & a_{11} \end{pmatrix} \begin{pmatrix} b_1 \\ b_2 \end{pmatrix}, \end{aligned} \tag{5}$$

where $N_{1,0}$ and $N_{2,0}$ are the stationary densities, and

$$det = a_{11}a_{22} - a_{12}a_{21} \tag{6}$$

is the determinant of the original matrix. From equation (5) one obtains the ratio of the excited to ground state densities,

$$\frac{N_{2,0}}{N_{1,0}} = \frac{a_{21}b_1 + a_{11}b_2}{a_{22}b_1 + a_{12}b_2}. \tag{7}$$

In principle, equation (3) may also have time-dependent solutions, but in appendix 3 we prove that eventually any such solution decays exponentially to the stationary point, equation (7).

3. Characterization of the Radiation Field

In the literature, astrophysical photoionizing plasmas are generally characterized by the ionization parameter, ξ,

$$\xi = \frac{L}{r^2 n_{\rm e}} \quad ({\rm units, erg\,cm\,s^{-1}}), \tag{8}$$

where L is the compact object's luminosity, r is its distance from the irradiated plasma, and $n_{\rm e}$ is the free-electron density. The measured values of ξ in astrophysical objects vary between 10 and 10^4.

In this paper we characterize the radiation field by two parameters: (i) the photon intensity, X_0, namely, the spectrum-integrated number of photons hitting the plasma per cm^2 per second, and (ii) the radiation temperature, $T_{\rm r}$, measured in eV, which determines the spectral shape of the incident radiation. More accurate definitions of these quantities are given in appendix 1.

X_0 is related to ξ by

$$\begin{aligned} X_0 &= \frac{L}{4\pi r^2 \langle h\nu \rangle} = \frac{\xi n_{\rm e}}{4\pi \langle h\nu \rangle}; \\ \langle h\nu \rangle &= \frac{\pi^4}{30\zeta(3)} T_{\rm r} = 2.701 T_{\rm r}. \end{aligned} \tag{9}$$

Here, $\langle h\nu \rangle$ is the average photon energy. In compact objects $200 \le T_{\rm r} \le 2000$ eV. It follows that the astrophysical values of X_0, therefore, vary between

$$1 \cdot 10^6 n_{\rm e} \le X_0 \le 1 \cdot 10^{10} n_{\rm e} \quad ({\rm photons\,cm^{-2}\,s^{-1}}). \tag{10}$$

Are these values sufficiently large to generate population inversion under astrophysical conditions? To answer this question we have to give an estimate to those values of X_0 that can generate overpopulation of the upper state.

4. High Radiation Field Approximation

Some arithmetics is inevitable. In photoionizing plasmas the material temperature is relatively low, about 10–50 eV, which means that the rates of the reactions induced by electron–ion interactions are very low. In particular, the rates of the electron impact ionization, excitation, and de-excitation as well as three-body and dielectronic recombinations may be safely neglected from the equations. Only the radiation-induced reactions and radiative recombinations have significantly large rates. Under such conditions, equations (A9)–(A11) and (A13)–(A15) reduce to the following simpler forms:

$$a_{11} = \Phi_{\rm He,K} + X_0\,\mathcal{L}_{\rm x}(E_{12})\,\Delta E_{12}\,h B_{\rm He,1\to 2} + n_{\rm e} R^{\rm (r)}_{\rm He,L}, \tag{11}$$

Downloaded from https://academic.oup.com/pasj/article-abstract/63/4/727/2902469
by Institute of Botany, CAS user
on 17 November 2017

$$a_{12} = A_{\mathrm{He},2\to1}, \tag{12}$$

$$b_1 = N_{\mathrm{Li}}\,\Phi_{\mathrm{Li,L}} + n_{\mathrm{e}}\,N_{\mathrm{H}}\,R^{(\mathrm{r})}_{\mathrm{H,K}}, \tag{13}$$

$$a_{21} = X_0\,\mathcal{L}_{\mathrm{x}}(E_{12})\,\Delta E_{12}\,h\,B_{\mathrm{He},1\to2}, \tag{14}$$

$$a_{22} = \Phi_{\mathrm{He,K}} + \Phi_{\mathrm{He,L}} + A_{\mathrm{He},2\to1} + n_{\mathrm{e}}\,(R^{(\mathrm{r})}_{\mathrm{He,K}} + R^{(\mathrm{r})}_{\mathrm{He,L}}), \tag{15}$$

$$b_2 = N_{\mathrm{Li}}\Phi_{\mathrm{Li,K}} + n_{\mathrm{e}}N_{\mathrm{H}}R^{(\mathrm{r})}_{\mathrm{H,L}}. \tag{16}$$

For the definitions of the various symbols see appendix 2. In equations (11)–(16) the symbol $R^{(2)}$ for the two-body recombination (radiative + dielectronic) was replaced by $R^{(\mathrm{r})}$, the rate coefficient for radiative recombination. Denote by x the ratio

$$x = \frac{b_1}{b_2} = \frac{N_{\mathrm{Li}}\Phi_{\mathrm{Li,L}} + n_{\mathrm{e}}N_{\mathrm{H}}R^{(\mathrm{r})}_{\mathrm{H,K}}}{N_{\mathrm{Li}}\Phi_{\mathrm{Li,K}} + n_{\mathrm{e}}N_{\mathrm{H}}R^{(\mathrm{r})}_{\mathrm{H,L}}}. \tag{17}$$

Using equations (11)–(17), equation (7) is transformed into (including a substitution $a' = \Phi_{\mathrm{He,K}} + n_{\mathrm{e}}\,R^{(\mathrm{r})}_{\mathrm{He,L}}$ for contraction of printed forms here)

$$\frac{N_{2,0}}{N_{1,0}} = \frac{a_{21}x + a_{11}}{a_{22}x + a_{12}} = \frac{(x+1)X_0\mathcal{L}_{\mathrm{x}}(E_{12})\Delta E_{12}hB_{\mathrm{He},1\to2} + a'}{(x+1)A_{\mathrm{He},2\to1} + x\,(a' + \Phi_{\mathrm{He,L}} + n_{\mathrm{e}}R^{(\mathrm{r})}_{\mathrm{He,K}})} \tag{18}$$

or, using equation (A7),

$$\frac{N_{2,0}}{N_{1,0}} = \frac{(x+1)X_0\,\mathcal{L}_{\mathrm{x}}(E_{12})\Delta E_{12}hc^2/(2h\nu^3)(g_1/g_2)A_{\mathrm{He},2\to1} + a'}{(x+1)A_{\mathrm{He},2\to1} + x\left(a' + \Phi_{\mathrm{He,L}} + n_{\mathrm{e}}\,R^{(\mathrm{r})}_{\mathrm{He,K}}\right)}. \tag{19}$$

5. Numerical Estimates

An analysis of equation (17) indicates that mostly $x \geq 1$ (because $R^{(\mathrm{r})}_{\mathrm{H,K}} > R^{(\mathrm{r})}_{\mathrm{H,L}}$, but $\Phi_{\mathrm{Li,L}} \gtreqless \Phi_{\mathrm{Li,K}}$, depending on the radiation temperature), although in some cases x can be somewhat smaller than 1.

As a first step, we carry out an analytical estimate of the value of equation (19) for the case of $x > 1$.

(i) $x > 1$

Clearly, for $x > 1$ the last term in the numerator of equation (19) are smaller than the last 3 terms in the denominator. Therefore, to satisfy the condition for overpopulation, equation (2), the first term of the numerator must be significantly larger than the first term in the denominator. Since both these terms have the factor $(x + 1)A_{\mathrm{He},2\to1}$ in common, the numerator will be larger than the denominator if

$$X_0\mathcal{L}_{\mathrm{x}}(E_{12})\Delta E_{12}hc^2/(2h\nu^3)(g_1/g_2) \gg 1. \tag{20}$$

We insert into equation (20) $g_1/g_2 = 1/3$, and $hc^2/(2h\nu^3) = 4\pi^3\hbar^3c^2/E^3_{12}$. Assuming that the line width is caused by Doppler broadening, then $\Delta E_{12}/E_{12} = \sqrt{2\ln 2\,T_{\mathrm{e}}/(A\,M_{\mathrm{a}}c^2)}$ (A is the atomic weight, and $M_{\mathrm{a}}c^2$ the atomic unit mass). With these identities condition (20) transforms into ($T_{\mathrm{e}} \simeq 50\,\mathrm{eV}$)

$$2.880\cdot10^{-27}\,(\mathrm{eV^3\,cm^2\,s})\;X_0\mathcal{L}_{\mathrm{x}}(E_{12})\frac{1}{E^2_{12}\sqrt{A}} \gg 1. \tag{21}$$

In other words, lasing is possible if

$$E^2_{12}\sqrt{A} \ll 3\cdot10^{-27}\frac{\mathrm{cm^2\ s\ eV}}{\mathrm{photon}}X_0\mathcal{L}_{\mathrm{x}}(E_{12}). \tag{22}$$

A plausible approximation for the $1s2p\,{}^1P_1 \to 1s^2\,{}^1S_0$ transition energy as function of the atomic number is $E_{12} = 6\,\mathrm{eV}\times Z^{2.1}$, valid between $3 \leq Z \leq 26$. Using $A \simeq 2\,Z$, and taking arbitrarily $\mathcal{L}_{\mathrm{x}}(E_{12}) = 0.1$, condition (22) for x-ray lasing becomes

$$X_0 \gg 1.8\cdot10^{29}\,Z^{4.7}\,\frac{\mathrm{photons}}{\mathrm{cm^2\ s\ eV}}. \tag{23}$$

A comparison of condition (23) with available astrophysical radiative intensities, condition (10), indicates that x-ray lasing is possible if and only if

$$Z^{4.7} \ll (5\cdot10^{-4} \to 3)\left(\frac{n_{\mathrm{e}}}{10^{20}\,\mathrm{cm^{-3}}}\right). \tag{24}$$

Even for a lithium plasma, $Z = 3$, this requires electron densities on the order of $n_{\mathrm{e}} \sim 5\cdot10^{21} \to 3\cdot10^{25}$ electrons cm^{-3}. At such tremendous electron densities the collisional processes dominate the plasma, and it cannot be a purely photoionizing one. Population inversion, therefore, is not possible. Varying the approximations of T_{e} and $\mathcal{L}_{\mathrm{x}}(E_{12})$ within reasonable limits cannot change this conclusion.

(ii) $x < 1$

To check that the above conclusions are valid also for $x < 1$, we built a computer code that calculates the ratio $N_{2,0}/N_{1,0}$ using equation (18). As the plasma material we have used nitrogen, which has both low Z, and a relatively high abundance in the Universe. Our computations confirmed the above conclusions for $x < 1$, too. In fact, the computed ratio of the excited to the ground state populations was never higher than 2%, even under artificially high irradiation conditions.

The physical reason for this result, as indicated by the computations, is the fact that He-like ions prevail only within a limited region of photon intensities, X_0. For higher intensities the plasma is fully ionized, while for lower intensities the ionization rate is not enough to achieve He-like ions. Although the limits depend on the radiation temperature, as a rule there are always limits on the intensity for which He-like ions are the most abundant species. Also, when using photon intensities of astrophysical relevance, within these limits the photoionization or photoexcitation rates are not sufficient to maintain a population inversion.

6. Discussion

In this paper we proved that, as long as we assume the Planckian radiation spectrum, there can be no x-ray lasing in astrophysical material for our model transition up to the presently known highest irradiation conditions from astrophysical objects. This result is in agreement with an initial intuition, because as the transition energy gap goes up so does the Einstein coefficient. The upper state decays, therefore, rapidly,

Downloaded from https://academic.oup.com/pasj/article-abstract/63/4/727/2902469
by Institute of Botany, CAS user
on 17 November 2017

and there is not enough time to build up a population inversion relative to the ground state. As a matter of fact, we only confirmed this intuitive description by rigorous methods.

Although our analysis refers to a very special transition only, our treatment is general enough to be related to other possible transitions as well. In fact, only in the last step, condition (23), did we use values specific to our model transition. Referring to condition (22), we see that the photon intensity, X_0, necessary to obtain population inversion depends only on the transition energy and the atomic weight, but not on the details of the atomic states involved in the transition. Equation (22) indicates that the population inversion can be maintained by lower irradiation intensities, X_0, if the transition energy is low and the atoms have low atomic weight. Actually, lasing from astrophysical objects has been observed in the near IR, although not in shorter wavelength regimes. Combining (22) with (10) one obtains a general condition for possible population inversion in astrophysical objects,

$$E_{12}^2\sqrt{A} \ll (0.03 \to 150)\,\mathrm{eV}^2 \times \frac{n_\mathrm{e}}{10^{20}\,\mathrm{cm}^{-3}}. \tag{25}$$

As a matter of fact, this condition can be fulfilled for $E_{12} \precsim$ 1–2 eV and a low atomic weight material in an atmosphere with an electron density of $n_\mathrm{e} < 10^{20}\,\mathrm{cm}^{-3}$. This is in general agreement with an analysis of Johansson and Letokhov. If higher irradiation conditions will be discovered, this limit can be pushed to shorter lasing wavelengths.

Finally, it should be noted that our conclusion strongly depends on the assumption of the Planckian radiation source. Sources having different spectral distributions (strong lines or other similar narrow distributions) may be more efficient in inducing population inversion. It will be interesting to repeat the above estimates when and if such radiation sources will be discovered.

Appendix 1. Rate Coefficient for Photoionization and Resonant Photoabsorption

In this paper the radiation field is assumed to have a Planckian distribution. The field is characterized by the photon distribution function, $X(h\nu)\,d(h\nu)$, which is the number of photons crossing a unit area in unit time. From $X(h\nu)$ we extract the normalized photon spectral profile function $\mathcal{L}_\mathrm{X}(h\nu)\,d(h\nu)$, $[\int \mathcal{L}_\mathrm{X}(h\nu)\,d(h\nu) = 1]$, such that

$$X(h\nu)\,d(h\nu) = X_0\mathcal{L}_\mathrm{X}(h\nu)d(h\nu), \tag{A1}$$

where $X_0 = \int X(h\nu)\,d(h\nu)$ is the total spectrum-integrated number of photons hitting the material per cm^2 per second. Then, for a black body radiator, which has temperature T_r,

$$\mathcal{L}_\mathrm{X}(h\nu)\,d(h\nu) = \frac{1}{2\zeta(3)T_\mathrm{r}^3} \times \frac{(h\nu)^2\,d(h\nu)}{\exp(h\nu/T_\mathrm{r})-1}, \tag{A2}$$

where $\zeta(3) = 1.2020$ is the Riemann zeta-function. To obtain the photoionization rate, this function has to be convoluted with the photoionization cross section,

$$\sigma_{\zeta,\mathrm{K}}(h\nu) = \begin{cases} \sigma_{\zeta,\mathrm{K},0}\left(\dfrac{B_{\zeta,\mathrm{K}}}{h\nu}\right)^{\gamma_\mathrm{K}} & \text{if } h\nu \geq B_{\zeta,\mathrm{K}} \\ 0 & \text{otherwise,} \end{cases} \tag{A3}$$

where $\sigma_{\zeta,\mathrm{K},0}$ is the cross section at the K-edge tip of an ion having charge ζ; $B_{\zeta,\mathrm{K}}$ is the corresponding binding energy; and γ_K is a dimensionless numbers ≤ 3, which defines the slope of the cross-section as a function of $h\nu$. A similar formula holds true for L-shell photoionization. The total rate for K-shell photoionization is, therefore,

$$\begin{aligned}\Phi_{\zeta,\mathrm{K}} &= \int_{B_{\zeta,\mathrm{K}}}^{\infty} X(h\nu)\,d(h\nu)\,\sigma_{\zeta,\mathrm{K},0}\left(\frac{B_{\zeta,\mathrm{K}}}{h\nu}\right)^{\gamma} \\ &= X_0\,\sigma_{\zeta,\mathrm{K},0}\,F_\gamma(B_{\zeta,\mathrm{K}}/T_\mathrm{r}),\end{aligned} \tag{A4}$$

where

$$F_\gamma(x) = \frac{1}{2\,\zeta(3)}\,x^\gamma \int_x^\infty \frac{y^{2-\gamma}\,dy}{e^y-1} \tag{A5}$$

is a dimensionless function that depends on the spectral shape of the incident radiation, but not on its intensity. A similar expression is obtained for L-shell ionization.

The rate of the resonant photoexcitation is given by Einstein's formula:

$$\begin{aligned}\frac{\text{transitions}}{\mathrm{cm}^3\cdot\mathrm{s}} &= N_{\zeta 1}\,hX\,(h\nu = E_{1\to 2})\,\Delta h\nu\,B_{\zeta,1\to 2} \\ &= N_{\zeta 1}\,hX_0\,\mathcal{L}_\mathrm{X}(E_{1\to 2})\,\Delta h\nu\;B_{\zeta,1\to 2}.\end{aligned} \tag{A6}$$

In equation (A6), $N_{\zeta 1}$ is the density of ground-state ions, and $\Delta h\nu$ is the transition width. [An extra h, Planck constant, is inserted into equation (A6) to account for the change of the B-coefficient from $\mathrm{cm}^2\,\mathrm{Hz}^{-1}\,\mathrm{s}^{-1}$ to $\mathrm{cm}^2\,\mathrm{eV}^{-1}\,\mathrm{s}^{-1}$.]

Appendix 2. Basic Rate Equation for the Ground and Excited States in He-Like Ions

The basic processes that populate and depopulate the He-like ground and excited states are the following tables 1, 2, 3, and 4 (see also figure 1):

The Einstein B-coefficient is related to the Einstein A-coefficient by

$$A_{2\to 1} = 2\frac{h\nu^3}{c^2}\,\frac{g_2}{g_1}\,B_{1\to 2}. \tag{A7}$$

Accounting for all of the above processes, the rate equation for the He-like g.s. is written as

$$\frac{dN_{\mathrm{He},1}}{dt} = b_1 - a_{11}N_{\mathrm{He},1} + a_{12}N_{\mathrm{He},2}, \tag{A8}$$

where

$$\begin{aligned}a_{11} &= \Phi_{\mathrm{He,K}} + X_0\,\mathcal{L}_\mathrm{x}(E_{12})\,\Delta E_{12}\,hB_{\mathrm{He},1\to 2} \\ &\quad + n_\mathrm{e}\left(I_{\mathrm{Li,K}} + \mathcal{E}_{\mathrm{He},1\to 2} + R^{(2)}_{\mathrm{He,L}} + n_\mathrm{e}R^{(3)}_{\mathrm{He,L}}\right),\end{aligned} \tag{A9}$$

$$a_{12} = A_{\mathrm{He},2\to 1} + n_\mathrm{e}\,D_{\mathrm{He},2\to 1}, \tag{A10}$$

$$b_1 = N_{\mathrm{Li}}\,(\Phi_{\mathrm{Li,L}} + n_\mathrm{e}\,I_{\mathrm{Li,L}}) + n_\mathrm{e}\,N_\mathrm{H}\left(R^{(2)}_{\mathrm{H,K}} + n_\mathrm{e}\,R^{(3)}_{\mathrm{H,K}}\right). \tag{A11}$$

It should be mentioned explicitly that a_{11}, a_{12}, and b_1 are all positive.

The corresponding processes for the excited 1s2p state are in table 3.

In a manner similar to the g.s., the rate equation for the excited state is written as

Downloaded from https://academic.oup.com/pasj/article-abstract/63/4/727/2902469
by Institute of Botany, CAS user
on 17 November 2017

Table 1. He-like $1s^2$ ground state, populating processes.

	Populating process	Initial state	Final state	Process rate ($cm^{-3}\ s^{-1}$)
(a)	Photoionization	Li-like	He-like g.s.	$N_{\rm Li}\,\Phi_{\rm Li,L}$
(b)	Collisional ionization	Li-like	He-like g.s.	$N_{\rm Li}\,n_{\rm e}\,I_{\rm Li,L}$
(c)	Spontaneous decay	He-like e.s.	He-like g.s.	$N_{\rm He,2}\,A_{\rm He,2\to1}$
(d)	Collisional de-excitation	He-like all e.s.	He-like g.s.	$n_{\rm e}N_{\rm He,2}D_{\rm He,2\to1}$
(e)	Two-body recombination	H-like g.s.	He-like g.s.	$n_{\rm e}N_{\rm H}\,R^{(2)}_{\rm H,K}$
(f)	Three-body recombination	H-like g.s.	He-like g.s.	$n_{\rm e}^2N_{\rm H}\,R^{(3)}_{\rm H,K}$

$N_{\rm Li}, N_{\rm H}$ — are the densities of Li- and H-like species, respectively.
$N_{\rm He,1}, N_{\rm He,2}$ — the densities of He-like species in the ground (g.s.) and excited (e.s) states, respectively.
$n_{\rm e}$ — electron density.
$\Phi_{\rm Li,L}$ — photoionization rate of a L-shell electron in Li-like species, see appendix 1.
$I_{\rm Li,L}$ — electron impact ionization rate coefficient (r.c.) of an L-shell electron in a Li-like ion.
$A_{\rm He,2\to1}$ — Einstein coefficient for the $1s2p\,^1P_1 \to 1s^2\,^1S$ spontaneous decay in He-like species.
$D_{\rm He,2\to1}$ — collisional de-excitation r.c. for the $1s2p\,^1P_1 \to 1s^2\,^1S$ transition.
$R^{(2)}_{\rm H,K}$ — two-body (radiative+dielectronic) recombination r.c. into the K-shell of H-like species.
$R^{(3)}_{\rm H,K}$ — three-body recombination r.c. into the K-shell of H-like species.

Table 2. He-like $1s^2$ ground state, depopulating processes.

	Depopulating process	Initial state	Final state	Process rate ($cm^{-3}\ s^{-1}$)
(a)	Photoionization	He-like g.s.	H-like g.s.	$N_{\rm He,1}\,\Phi_{\rm He,K}$
(b)	Collisional ionization	He-like g.s.	H-like g.s.	$4n_{\rm e}\,N_{\rm He,1}\,I_{\rm Li,K}$
(c)	Resonant photoabsorption	He-like g.s.	He-like e.s.	$N_{\rm He,1}X_0\,\mathcal{L}_{\rm x}(E_{12})$ $\times\Delta E_{12}\,h\,B_{\rm He,1\to2}$
(d)	Collisional excitation	He-like g.s.	He-like e.s.	$n_{\rm e}\,N_{\rm He,1}\,\mathcal{E}_{\rm He,1\to2}$
(e)	Two-body recombination	He-like g.s.	Li-like g.s.	$n_{\rm e}N_{\rm He,1}\,R^{(2)}_{\rm He,L}$
(f)	Three-body recombination	He-like g.s.	Li-like g.s.	$n_{\rm e}^2N_{\rm He,1}\,R^{(3)}_{\rm He,L}$

E_{12} — the energy difference between the $1s\,2p\,^1P_1$ and $1s^2\,^1S$ states.
ΔE_{12} — the transition line width.
$\mathcal{L}_{\rm x}(E_{12})$ — the value of the photon distribution profile function for $E = E_{12}$.
$B_{\rm He,1\to2}$ — the Einstein B-coefficient for g.s. to e.s. transition, units: $cm^2\,(eV^{-1}\ s^{-1})$, see appendix 1.

Table 3. He-like 1s2p excited state, populating processes.

	Populating process	Initial state	Final state	Process rate ($cm^{-3}\ s^{-1}$)
(a)	Photoionization	Li-like	He-like e.s.	$N_{\rm Li}\,\Phi_{\rm Li,K}$
(b)	Collisional ionization	Li-like	He-like e.s.	$N_{\rm Li}\,n_{\rm e}\,I_{\rm Li,K}$
(c)	Resonant photoabsorption	He-like g.s.	He-like e.s.	$N_{\rm He,1}X_0\,\mathcal{L}_{\rm x}(\Delta E_{12})$ $\times\Delta E_{12}h\,B_{\rm He,1\to2}$
(d)	Collisional excitation	He-like g.s.	He-like e.s.	$n_{\rm e}\,N_{\rm He,1}\,\mathcal{E}_{\rm He,1\to2}$
(e)	Two-body recombination	H-like g.s.	He-like e.s.	$n_{\rm e}N_{\rm H}\,R^{(2)}_{\rm H,L}$
(f)	Three-body recombination	H-like g.s.	He-like e.s.	$n_{\rm e}^2N_{\rm H}\,R^{(3)}_{\rm H,L}$

Table 4. He-like 1s2p excited state, depopulating processes.

	Depopulating process	Initial state	Final state	Process rate ($cm^{-3}\ s^{-1}$)
(a)	Photoionization	He-like e.s.	H-like ion	$N_{\rm He,2}\,(\Phi_{\rm He,K}+\Phi_{\rm He,L})$
(b)	Collisional ionization	He-like e.s.	H-like g.s.	$n_{\rm e}\,N_{\rm He,2}I_{\rm Li,L}$
(c)	Spontaneous decay	He-like e.s.	He-like g.s.	$N_{\rm He,2}A_{\rm He,2\to1}$
(d)	Collisional de-excitation	He-like e.s.	He-like g.s.	$n_{\rm e}\,N_{\rm He,2}\,\mathcal{D}_{\rm He,2\to1}$
(e)	Two-body recombination	He-like e.s.	Li-like ion	$n_{\rm e}N_{\rm He,2}(\,R^{(2)}_{\rm He,L}+R^{(2)}_{\rm He,K})$
(f)	Three-body recombination	He-like e.s.	Li-like ion	$n_{\rm e}^2N_{\rm He,2}\,(R^{(3)}_{\rm He,L}+R^{(3)}_{\rm He,K})$

Downloaded from https://academic.oup.com/pasj/article-abstract/63/4/727/2902469
by Institute of Botany, CAS user
on 17 November 2017

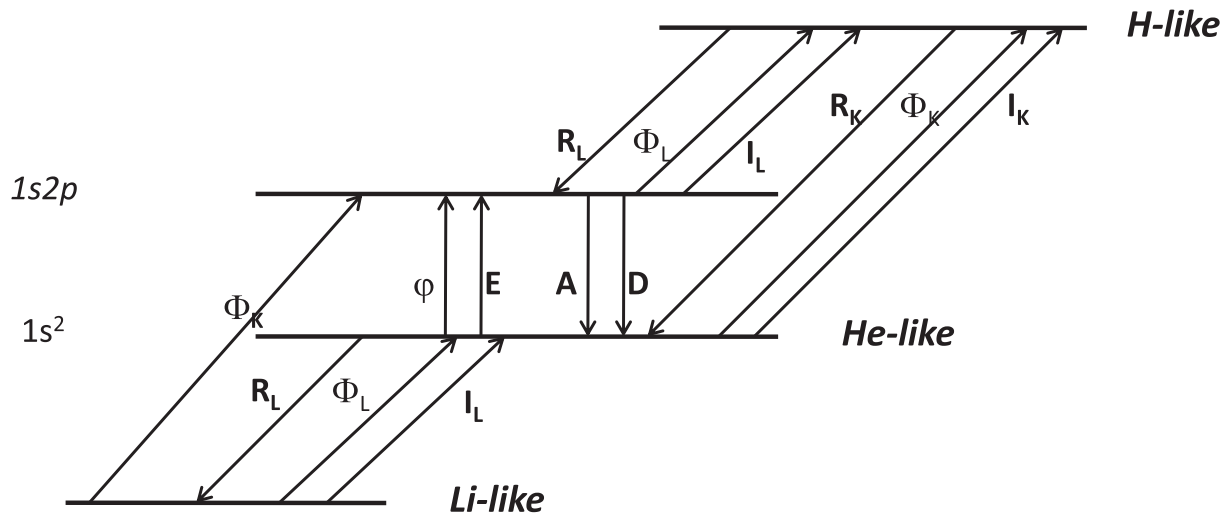


Fig. 1. Processes that populate and depopulate the $1s^2$ ground and 1s2p excited states of helium-like species. The notations in the figure are the following: R — recombination (including radiative, dielectronic, and 3-body recombinations); I — electron impact ionization; Φ — photoionization; E — electron impact excitation; D — electron impact de-excitation; A — spontaneous decay; φ — resonant photoexcitation. The K- or L-subscripts correspond to the atomic shell of the electron subjected to the process.

$$\frac{dN_{\mathrm{He},2}}{dt} = b_2 + a_{21} N_{\mathrm{He},1} - a_{22} N_{\mathrm{He},2}, \tag{A12}$$

where

$$a_{21} = X_0 \mathcal{L}_{\mathrm{x}}(\Delta E_{12})\, \Delta E_{12}\, h B_{\mathrm{He},1\to 2} + n_{\mathrm{e}} \mathcal{E}_{\mathrm{He},1\to 2}, \tag{A13}$$

$$a_{22} = \Phi_{\mathrm{He,K}} + \Phi_{\mathrm{He,L}} + A_{\mathrm{He},2\to 1} + n_{\mathrm{e}} \Big[I_{\mathrm{Li,L}} + \mathcal{D}_{\mathrm{He},2\to 1} + (R^{(2)}_{\mathrm{He,K}} + n_{\mathrm{e}} R^{(3)}_{\mathrm{He,K}}) + (R^{(2)}_{\mathrm{He,L}} + n_{\mathrm{e}} R^{(3)}_{\mathrm{He,L}}) \Big], \tag{A14}$$

$$b_2 = N_{\mathrm{Li}} (\Phi_{\mathrm{Li,K}} + n_{\mathrm{e}} I_{\mathrm{Li,K}}) + n_{\mathrm{e}} N_{\mathrm{H}} (R^{(2)}_{\mathrm{H,L}} + n_{\mathrm{e}} R^{(3)}_{\mathrm{H,L}}). \tag{A15}$$

Again, the three numerical coefficients are all positive.

Equations (A8) and (A12) can be rewritten in matrix form as

$$\frac{d}{dt}\mathcal{N} = \mathcal{A}\mathcal{N} + \mathcal{B}, \tag{A16}$$

where

$$\mathcal{N} = \begin{bmatrix} N_1(t) \\ N_2(t) \end{bmatrix}, \quad \mathcal{B} = \begin{pmatrix} b_1 \\ b_2 \end{pmatrix} \text{ and, } \quad \mathcal{A} = \begin{pmatrix} -a_{11} & a_{12} \\ a_{21} & -a_{22} \end{pmatrix}. \tag{A17}$$

The stationary solution, $\mathcal{N}(t) = \mathcal{N}_0$, is obtained by substituting $(d/dt)\mathcal{N} = 0$ into equation (A16). The formal solution is

$$\mathcal{N}_0 = -\mathcal{A}^{-1}\mathcal{B}. \tag{A18}$$

Appendix 3. Proof that Time-Dependent Solutions of the Rate Equations Decay to the Stationary Point

In principle, equation (A16) may also have time-dependent solutions, $\mathcal{N}(t)$, different from the stationary one. For any such time-dependent solution, we denote by $\mathcal{M}(t)$ its difference from the stationary one,

$$\mathcal{M}(t) = \mathcal{N}(t) - \mathcal{N}_0. \tag{A19}$$

Inserting this into equation (A16) one obtains

$$\frac{d}{dt}\mathcal{M} = \mathcal{A}\mathcal{M}. \tag{A20}$$

Using a trial solution of the form $\mathcal{M}(t) = \mathcal{M}_0\, e^{\alpha t}$, equation (A20) reduces to

$$\alpha\mathcal{M} = \mathcal{A}\mathcal{M}, \tag{A21}$$

which becomes an eigenvalue problem for the matrix $\mathcal{A}$,

$$\begin{vmatrix} -a_{11} - \alpha & a_{12} \\ a_{21} & -a_{22} - \alpha \end{vmatrix} = 0. \tag{A22}$$

The eigenvalues of this quadratic equation are given by

$$\alpha_{1,2} = -\frac{a_{11} + a_{22}}{2} \left[1 \pm \sqrt{1 - \frac{4(a_{11}a_{22} - a_{12}a_{21})}{(a_{11} + a_{22})^2}} \right]. \tag{A23}$$

Using the explicit values for the matrix elements, equations (A11)–(A16), after lengthy algebra it can be shown that the term $4(a_{11}a_{22} - a_{12}a_{21})$ in the discriminant is positive and always smaller than $(a_{11} + a_{22})^2$. It turns out that the factor in the square root sign is positive and smaller than 1. This implies that the factor in the curly parentheses is always positive. Since $a_{11} + a_{22}$ is positive, it follows that both eigenvalues, $\alpha_{1,2}$, are real and negative. Therefore, $\mathcal{M}(t) \propto e^{-|\alpha| t}$, which means that $\mathcal{N}(t)$ always decays exponentially to the stationary point,

$$\mathcal{N}(t) = \mathcal{N}_0 + \mathcal{M}_0\, e^{-|\alpha| t}. \tag{A24}$$

Downloaded from https://academic.oup.com/pasj/article-abstract/63/4/727/2902469
by Institute of Botany, CAS user
on 17 November 2017

References

Bambynek, W., Crasemann, B., Fink, R. W., Freund, H.-U., Mark, H., Swift, C. A., Price, R. E., & Rao, P. V. 1972, Rev. Mod. Phys., 44, 716
Johansson, S., & Letokhov, V. S. 2007, New Astron. Rev., 51, 443
Messenger, S. J., & Strelnitski, V. 2010, MNRAS, 404, 1545
Nakai, N., Inoue, M., & Miyoshi, M. 1993, Nature, 361, 45
Porter, J. L., et al. 1992, Phys. Rev. Lett., 68, 796
Remington, B. A., Drake, R. P., & Ryutov, D. D. 2006, Rev. Mod. Phys., 78, 755
Stahler, S. W., & Palla, F. 2004, The Formation of Stars (New York: Wiley)
Takabe, H. 2001, Prog. Theor. Phys. Suppl., 143, 202
Wardle, M., & Yusef-Zadeh, F. 2002, Science, 296, 2350
Weaver, H., Williams, D. R. W., Dieter, N. H., & Lum, W. T. 1965, Nature, 208, 29
Weisberg, J. M., Johnston, S., Koribalski, B., & Stanimirović, S. 2005, Science, 309, 106
Whiteoak, J. B., & Gardner, F. F. 1973, Astrophys. Lett., 15, 211

Downloaded from https://academic.oup.com/pasj/article-abstract/63/4/727/2902469
by Institute of Botany, CAS user
on 17 November 2017